Journal of Nano- and Electronic Physics
Vol. **18** No 1, 01011(5pp) (2026)

Журнал нано- та електронної фізики
Том **18** № 1, 01011(5cc) (2026)

OPEN ACCESS

REGULAR ARTICLE

An *ab initio*-Based Computational Scheme for Description the Kinetic Properties of Wurtzite Zinc Oxide

O.P. Malyk*

Lviv Polytechnic National University, 79013 Lviv, Ukraine

(Received 12 September 2025; revised manuscript received 20 February 2026; published online 25 February 2026)

For the first time, the present study proposes an *ab initio*-based methodology for the determination of kinetic characteristics in wurtzite zinc oxide. The transport properties of material are analyzed within a rigorously developed short-range interaction models, which account the electron scattering processes induced by diverse types of crystal defects. Within the framework of density functional theory, the transition probabilities for electron scattering on lattice defects were determined employing numerically derived eigenfunctions together with a self-consistent crystal potential. This approach enabled the elimination of fitting parameters for six electron scattering mechanisms. The selection of zinc and oxygen pseudopotentials ensuring improved agreement between theoretical and experimental kinetic characteristics of ZnO over 3÷400 K is outlined. It has been proven that short-range models reproduce experimental results more accurately than long-range models.

Keywords: Wurtzite zinc oxide, DFT wave function, Electron transport, Point defects.

DOI: 10.21272/jnep.18(1).01011 PACS numbers: 72.10. – d; 72.10.Di; 72.10.Fk

1. INTRODUCTION

ZnO is a semiconductor with broad applications in device technologies. It is highly resistant to high-energy radiation, which makes it well-suited for space use [1]. It can also act as a substrate for the epitaxial growth of GaN films [2] and shows strong potential for spintronics applications [3]. While polycrystalline material suffices for most applications, recent progress in the growth of large-area single crystals has opened new prospects for blue and UV light emitters as well as for high-temperature, high-power transistors. Effective optimization and development of ZnO-based devices requires a detailed and correct description of the parameters of this material. References [1, 4-12] provide experimental data on transport phenomena in wurtzite ZnO as well as theoretical analyses carried out by different techniques. To analyze these data theoretically, the relaxation time approximation [6, 7], the variational method [11], and the Monte Carlo technique [12] were employed. The aforementioned methods are based on long-range scattering models, the limitations of which have been addressed in the author's previous works [13-15]. These works introduced an alternative framework for the description of transport phenomena, based on applying the short-range principle to electron-defect interactions in the crystal lattice. However, the short-range scattering models proposed by the author exhibit a limitation in that they require the use of fitting parameters. This article presents an approach for eliminating fitted parameters based on the electron wave function and self-consistent potential in a wurtzite-structured crystal, calculated within the density functional theory – generalized gradient approximation (DFT-GGA) framework, suggested by Perdew, Burke and Ernzerhof via the ABINIT code. The paper also establishes criteria for selecting the initial pseudopotentials of zinc and oxygen, which are used to calculate the wave function and crystal potential and ensure more better agreement between the theoretical and experimental temperature dependences of ZnO's kinetic coefficients.

2. ZINC AND OXYGEN PSEUDOPOTENTIALS SELECTION

Using the AtomPAW v4.2.0.3 code, Zn and O pseudopotentials were derived. During pseudopotential creation, the valence states $4s^2 4p^0 3d^{10}$ (Zn) and $2s^2 2p^4$ (O) were included. The physical values of the radius of the augmentation sphere R_{PAW} for zinc and oxygen were established based on the following criteria: a) the energy spectrum calculated using selected pseudopotentials at a given R_{PAW} reproduces the bandgap in agreement with experiment; b) determination of the dependence of electron mobility versus temperature using certain R_{PAW} values leads to agreement between theory and experiment. The analysis shows that these two criteria are satisfied by the radii value $R_{PAW} = 2.009$ for zinc and $R_{PAW} = 1.75$ for oxygen. Thus, these criteria enable the extraction of the physically meaningful wave function and crystal potential from among all mathematically possible ones.

* Correspondence e-mail: omalyk@ukr.net

Cite this article as: O.P. Malyk, *J. Nano- Electron. Phys.* 18 No 1, 01011 (2026) https://doi.org/10.21272/jnep.18(1).01011

3. THE DEPENDENCE OF WAVE FUNCTION AND CRYSTAL POTENTIAL VERSUS TEMPERATURE

The pseudopotentials, established in the previous section, allow us to determine the characteristics of ZnO, namely, the electron spectrum, its wave function, and the crystal potential. According to the results of the author's work [16], these characteristics of the semiconductor were expressed by a combination of the Zn and O pseudopotentials with the Hartree-Fock exchange potential. In the ABINIT code formalism, this combination is defined by the variable "exchmix". Variation of this parameter allows change the band gap value at the Γ point in wurtzite ZnO. Hence, the "exchmix" parameter can be chosen so that the theoretical band gap equals the experimental one. The calculation was performed for different types of supercells, while adjusting the exchmix parameter to obtain values of Eg corresponding to temperatures 0 and 300 K. As a result, the values exchmix = 0.95988 (0 K) and exchmix = 0.94502 (300 K) were obtained for the $1 \times 1 \times 1$ supercell, and the values exchmix = 0.88744 (0 K) and exchmix = 0.86068 (300 K) were obtained for the $2 \times 2 \times 1$ supercell. For each supercell, distinct numerically defined electron wave functions and crystal potentials are obtained at the specified temperatures of 0 or 300 K. This implies that the aforementioned method can be applied to derive the temperature dependence of these crystal properties, while ensuring that the theoretical band gap of the crystal agrees with its experimental value.

4. SHORT-RANGE ELECTRON SCATTERING MODELS IN WURTZITE SEMICONDUCTOR

Because the unit cell of wurtzite ZnO consists of four atoms (two Zn and two O), group theory allows the vibrations of this crystal to be expressed by the sum of irreducible representations: $\Gamma = 2A_1 + 2B_1 + 2E_1 + 2E_2$. The acoustic vibrations include a single A1 mode and one doubly E_1 mode. The optical branches of oscillations are the remaining irreducible representations $\Gamma_{\text{opt}} = A_1 + 2B_1 + E_1 + 2E_2$. The classification of these branches is based on whether the atomic displacements occur along the c_0-axis or in the perpendicular direction. It can be concluded that modes A_1 and E_1 represent polar optical (PO) oscillations, while modes $B_1^{(1)}$, $B_1^{(2)}$, $E_2^{(1)}$ and $E_2^{(2)}$ represent nonpolar optical (NPO) oscillations.

Ref. [16] reported, within an ab initio framework for a sphalerite semiconductor and invoking the short-range principle, that the electron-PO phonon scattering probability is proportional to the square of the quantity:

$$A_{PO} = \int \psi^* \left(R^2 - r^2/3\right) \psi \, d\mathbf{r}. \tag{1}$$

R denotes the range of the spherically symmetric interaction potential expressed in Cartesian coordinates. Given that the wurtzite unit cell includes two ZnO dipoles, formula (1) is applied to both. The integration region is the dipole-containing volume, defined by the zero-gradient condition of the crystal potential. The integral is calculated by switching to an oblique coordinate system using a known transition matrix. Thus, upon transformation the elementary cell becomes a unit cube, with the atom-pair volumes defined as follows: Zn_1–O_1(region I) – triangular rectangular prism; Zn_2–O_2(region II) – square rectangular prism. The value of R is determined by the average value of the radius of the inscribed and circumscribed sphere for regions I and II. This gives $R_{\text{I}} = 2.336$ Å and $R_{\text{II}} = 2.1495$ Å.

Given the temperature dependence of the electron wave function, the results for regions I and II inherit the same dependence. Under the assumption of linearity with temperature, the electron-PO phonon scattering yields:

$$\begin{aligned} A_{PO}{}^2 &= A_{PO\ \mathrm{Zn_1O_1}}{}^2 + A_{PO\ \mathrm{Zn_2O_2}}{}^2; \\ A_{PO} &= \left(1.65 + 8.28\times10^{-6}\ \mathrm{T}\right) \times 10^{-20} m^2. \end{aligned} \tag{2}$$

Given the value of A_{PO}, the expressions for electron transition probabilities from state $\mathbf{k}$ to state $\mathbf{k}'$ under interaction with a polar optical phonon associated with the A_1 and E_1 modes can be derived.

The description of the electron-NPO interaction is based on the optical deformation potential, which in the case of the wurtzite ZnO is represented by different constants for different NPO modes. In analogy with PO-scattering, the model presumes sequential carrier interaction with two dipoles $d^2 = d_{Ga1N1}^2 + d_{Ga2N2}^2$, consistent with the short-range principle. For each $B_1^{(1)}$ and $B_1^{(2)}$ modes (oscillation along the c_0-axis) we will get only z-component, while for the $E_2^{(1)}$and $E_2^{(2)}$ modes (oscillation perpendicular to c_0-axis) we will obtain the x- and y-components of the optical deformation potential:

$$\text{mode } B_1^{(1)} - d_z = 1.45 - 1.48\times10^{-5}\,\mathrm{T\,eV}; \tag{3a}$$

$$\text{mode } B_1^{(2)} - d_z = 1.33 - 7.03\times10^{-6}\,\mathrm{T\,eV}; \tag{3b}$$

$$\text{mode } E_2^{(1)} - d_x = 1.35 + 2.2\times10^{-5}\,\mathrm{T\,eV}; \tag{3c}$$

$$\text{mode } E_2^{(1)} - d_y = 1.69 + 2.81\times10^{-5}\,\mathrm{T\,eV}; \tag{3d}$$

$$\text{mode } E_2^{(2)} - d_x = 3.43 + 4.4\times10^{-5}\,\mathrm{T\,eV}; \tag{3e}$$

$$\text{mode } E_2^{(2)} - d_y = 3.87 + 5.02\times10^{-5}\,\mathrm{T\,eV}. \tag{3f}$$

On the basis of the d values, one can derive the analytical expressions for electron transition probabilities between quantum states under the interaction with NPO phonons.

The scattering of electrons by acoustic (AC) phonons is described through three constants (deformation acoustic potentials), connected with two transverse and one longitudinal branches of acoustic oscillations. In regions I and II for these three branch of oscillations we have:

$$\begin{aligned} &E_{AC\parallel} = c_0/a_0 \times \left(0.1885 c_0 I_x + 0.0628\sqrt{3} c_0 I_y + 0.1885 a_0 I_z\right), \\ &E_{AC\perp x} = 0.09425\,\mathrm{c_0\ I_x}\,, E_{AC\perp y} = 0.09425\,\mathrm{c_0\ I_y}; \\ &I_x = \int_{I(II)} \psi^* V_x \psi \, d\mathbf{r}'; I_y = \int_{I(II)} \psi^* V_y \psi \, d\mathbf{r}'; I_z = \int_{I(II)} \psi^* V_z \psi \, d\mathbf{r}', \end{aligned} \tag{4}$$

where the components $\boldsymbol{V}$ are defined elsewhere [16]. Because the wave function and the self-consistent crystal potential are temperature depended, for the acoustic deformation constants one can obtain:

$$E_{AC\|} = 1.52 + 2.88\times10^{-5}\ \mathrm{T}\ \ \mathrm{eV}; \quad (5a)$$

$$E_{AC\perp x} = 0.30 + 2.95\times10^{-6}\ \mathrm{T}\ \ \mathrm{eV}; \quad (5b)$$

$$E_{AC\perp y} = 0.66 + 8.15\times10^{-6}\ \mathrm{T}\ \ \mathrm{eV}; \quad (5c)$$

Zinc oxide possesses strong piezoelectric properties, which can be represented by the tensor equation:

$$P_i = e_{ijk}\cdot S^{jk}, \quad (6)$$

where P_i – crystal polarization vector, e_{ijk} – piezoelectric tensor, S^{jk} – macroscopic deformation tensor. It is established that, in crystals with a wurtzite structure, the tensor e_{ijk} assumes the following form:

$$e_{ijk} = \begin{pmatrix} 0 & 0 & 0 & 0 & e_{15} & 0 \\ 0 & 0 & 0 & e_{15} & 0 & 0 \\ e_{13} & e_{13} & e_{33} & 0 & 0 & 0 \end{pmatrix}. \quad (7)$$

Employing Voigt's notation [17], this expression can be equivalently written in coordinate form as: $e_{13} = e_{133}$; $e_{33} = e_{333}; e_{15} = e_{113}$; other components $e_{ijk} = 0$. It follows that only components $P_i(i = 1,3)$ exist:

$$P_1 = e_{133}\,S^{33} + 2\,e_{113}\,S^{13}; \mathrm{P}_3 = e_{333}\,S^{33}. \quad (8)$$

Using the approach of [15], it can be established that the electron-piezoacoustic (PAC) phonon interaction is described by relation (1). Then, this type of interaction depends on temperature according to (2).

The ionized impurity scattering describe by the constant:

$$A_{ID} = \int_{\Omega} \Psi^{*}\Psi\times 1/\mathrm{r}\ \ d\mathbf{r}, \quad (9)$$

and the corresponding temperature dependence has the following form:

$$A_{ID} = \left(0.63 + 1.93\times10^{-7}\ \mathrm{T}\right)\times10^{10}\ \mathrm{m}^{-1}. \quad (10)$$

Two more scattering mechanisms, neutral impurity scattering (NI) and static strain center scattering (SS), are independent of temperature and are described in [15].

5. ANALYSIS OF INTRINSIC DEFECT STRUCTURES IN ZINC OXIDE

At a given temperature, the structure of intrinsic defects in ZnO was examined through a comparison between the energy spectra of ideal supercells ($1\times1\times1$, $2\times2\times1$) and those containing defects. For the calculation of the energy spectra of defective supercells, the "exchmix" parameter was assigned the value used for the respective ideal supercell. The method outlined in [16] was employed to calculate the ionization energy of defects. Given that the energy spectra of ideal and defective supercells are calculable at $T = 0$ K and $T = 300$ K, the ionization energies of defects at these temperatures can be derived. On the basis of a linear approximation, the temperature dependence of defect ionization energies can be established. The donor defect was selected on the grounds that its ionization energy is the lowest, guaranteeing its prevailing impact on charge transport in ZnO. An analysis of the type of defects in $1\times1\times1$ and $2\times2\times1$ supercells shows that the defect that satisfies the above condition is the $2\times2\times1$ supercell defect, which has the following structure:

$$Zn_{O2} + Zn_{O4} + Zn_{O6} + V_{O7} + V_{O8}. \quad (11)$$

The results of the calculation demonstrate that the relation between the defect ionization energy and temperature is given by:

$$E_d = 0.0844 + 1.649\times10^{-4}\ \mathrm{T}\ \ \mathrm{eV}. \quad (12)$$

From this, for $T = 0$ K and $T = 300$ K, we obtain, respectively, for the ionization energy $E_d = 84.4$ meV and $E_d = 34.9$ meV. These values of E_d are close to the values obtained in [6, 7] for two types of defects (deep and shallow donors), the nature of which is unknown. In our work, we propose an intrinsic defect, the energy range of which overlaps with the values in [6, 7].

6. VALIDATION OF THEORY BY EXPERIMENT

Given the structure of intrinsic defects, the electroneutrality equation can be expressed as:

$$n - p = N_d / \left\{1 + 2\exp\left[\left(F - E_d\right)/\left(k_B T\right)\right]\right\}, \quad (13)$$

where F denotes the Fermi level, and N_d represents the impurity donor concentration. For the purpose of Fermi level calculation, the subsequent characteristics of the crystal defect structure were employed: $N_d = 1\times10^{17}$ cm^{-3}, concentration of static strain center $N_{ss} = 1.4\times10^{13}\ \mathrm{cm}^{-3}$.

The electron mobility, as a key kinetic characteristic of the semiconductor, was computed based on the short-range scattering models introduced earlier, within the framework of the exact analytical solution of Boltzmann's equation [18]. The zinc oxide parameters employed in the calculations are reported in [15].

Theoretical predictions for the temperature dependence of electron mobility, based on short-range scattering models (solid line in Fig. 1), were evaluated against experimental data from [6, 7]. The experimental data presented here relate to ZnO specimen exhibiting the highest degree of perfection realized thus far. Furthermore, Fig. 1 illustrates a comparison of two conceptual approaches to transport phenomena in semiconductors: (a) the short-range scattering model and (b) the long-range scattering model, the latter treated within the relaxation-time approximation.

It is evident that the theoretical curve 1 provides a satisfactory agreement with the experimental data. At lower temperatures, theoretical curve 1 and the experimental data diverge, with the difference appearing as a shift along the temperature axis. A possible explanation lies in the incompleteness of the SS-scattering model, as it may need to account for the angular dependence of the interaction potential. On Fig. 1, dependences 2 and 3 are obtained within the relaxation

time approximation (elastic scattering): curve 2

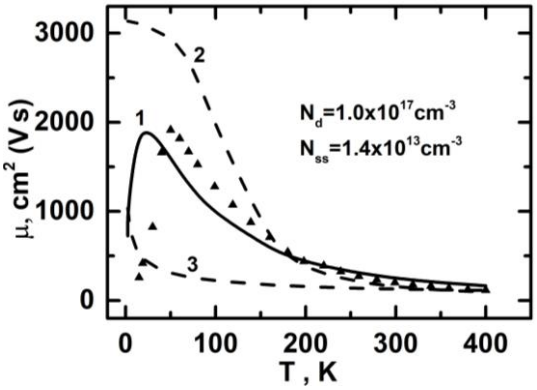

Fig. 1 – The electron mobility-temperature relationships in ZnO derived from two theoretical approaches

corresponds to the low-temperature regime, where the inequality $T << \theta_D$ (θ_D –Debye temperature for ZnO) is satisfied, while curve 3 represents the high-te-mperature regime, where the opposite inequality $T >> \theta_D$ holds. It is evident that curves 2 and 3 show both qualitative and quantitative deviations from the experimental data. From the literature, it is known that the Debye temperature for zinc oxide is approximately equal to $\theta_D = 400 \div 440$ K [19, 20]. This indicates that for zinc oxide, the low-temperature region corresponds to $T_{low} < 40 \div 44$ K, while the high-temperature region is defined by $T_{high} > 4000 \div 4400$ K, which is significantly higher than its melting point, $T_m = 2247$ K. Therefore, curve 3 is not suitable for representing the transport phenomena in a ZnO crystal in high-temperature region. Moreover, curve 2 is not applicable at temperatures above 40÷44 K, because in this range the scattering of optical phonons is no longer elastic. Conversely, short-range scattering models make it possible to account for the inelastic nature of electron-phonon interactions. Thus, it may be concluded that short-range scattering models provide a more accurate description of electron scattering on defects within the zinc oxide crystal lattice.

The impact of different scattering mechanisms on temperature dependence of electron mobility is depicted in Fig. 2. At low temperatures (T < 40-44 K), SS-scattering is observed to be the dominant scattering mechanism in the ZnO sample. For temperatures above 10 K, NI and PAC scattering mechanisms start to contribute. Above 80 K, the predominant scattering process is PAC scattering, which reflects the strong pie zoelectric behavior of zinc oxide. In the temperature regime $T > 300$ K, the PO scattering mechanism becomes comparable in significance to the PAC mechanism. The contribution of the remaining scattering mechanisms is insignificant.

The short-range scattering models under consideration enable the determination of the temperature dependence of the electron Hall factor, as illustrated in Fig. 3. This dependence display minima, the positions of which are governed by the defect concentration. This behavior arises from the transition between the temperature regime dominated by a single scattering mechanism, specifically the SS mechanism, and the regime where a combined scattering mechanism (PAC and PO) becomes significant.

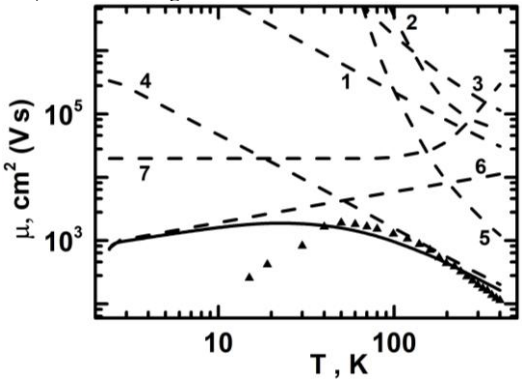

Fig. 2 – Contribution of individual scattering mechanisms to electron mobility in ZnO. The solid line shows the combined (mixed) mechanism. Curves 1 through 7 represent AC, ID, NPO, PAC, PO, SS, and NI scattering, respectively.

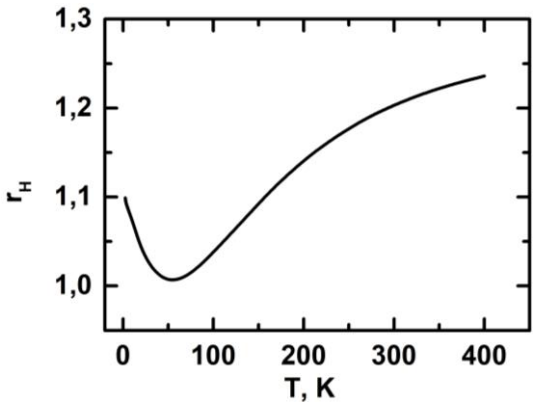

Fig. 3 – Variation of the electron Hall factor with temperature in zinc oxide

7. CONCLUSIONS

Based on the findings of this study, the following conclusions are established:

a) A procedure is suggested for choosing Zn and O pseudopotentials that ensures close agreement between theoretical predictions and experimental results.

b) A procedure is proposed for evaluating the temperature dependence of the electron wave function and potential energy in wurtzite-structured ZnO.

c) Seven models of short-range electron scattering on lattice defects in wurtzite-structured ZnO are presented.

d) The structure of an intrinsic defect in wurtzite-structured ZnO, which predominantly influences charge transport, has been investigated, and the temperature dependence of its ionization energy has been determined.

e) A reasonably strong consistency has been demonstrated between the theoretical temperature dependence of electron mobility and the experimental observations for the ZnO sample with a wurtzite structure.

f) It has been shown that the author's proposed method for describing transport phenomena in ZnO provides a more accurate representation of electron scattering by crystal lattice defects than approaches based on long-range scattering models.

g) The contributions of different scattering mechanisms to electron mobility were identified in the temperature

range of 3-400 K, and the temperature dependence of the electron Hall factor within the same range was calculated.
h) The suggested approach for evaluating kinetic characteristics is applicable to other semiconductors possessing a wurtzite structure.
i) It is worth emphasizing that the proposed approach for describing electron–phonon interactions is also applicable to semiconductors with more complex unit cell structures.

REFERENCES

1. D.C. Look, D.C. Reynolds, JW. Hemski, R. L. Jones, J.R. Sizelove, *Appl. Phys. Lett.* **75**, 811 (1999).
2. X. Gu, M.A. Reshchikov, A. Teke, D. Johnstone, H. Morkoc, B. Nemeth, J. Nause, *Appl. Phys. Lett.* **84**, 2268 (2004).
3. S.J. Pearton, W.H. Heo, M. Ivill, D.P. Norton, T. Steiner, *Semicond. Sci. Technol.* **19**, R59 (2004).
4. A.R. Hutson, *J. Phys. Chem. Solids* **8**, 467 (1959).
5. D.L. Rode, *Semiconductors and Semimetals* Vol. 10, Chap. 1 (Eds. by R.K. Willardson, A.C. Beer) (New York, San Francisco, London: Academic Press: 1975).
6. D.C. Look, D.C. Reynolds, J.R. Sizelove, R.L. Jones, C.W. Litton, G. Cantwell, W.C. Harsch, *Solid Stat Commun.* **105**, 399 (1998).
7. D.C. Look, *Mater. Sci. Eng. B* **80**, 383 (2001).
8. T. Edahiro, N. Fujimura, T. Ito, *J. Appl. Phys.* **93**, 7673 (2003).
9. H. Kato, M. Sano, K. Miyamoto, T. Yao, *Jpn. J. Appl. Phys.* **42**, 2241 (2003).
10. K. Miyamoto, M. Sano, H. Kato, T. Yao, *J. Cryst. Growth* **265**, 34 (2004).
11. T. Makino, Y. Segawa, A. Tsukazaki, A. Ohtomo, M. Kawasaki, *Appl. Phys. Lett.* **87**, 022101 (2005).
12. J.D. Albrecht, P.P. Ruden, S. Limpijumnong, W.R.L. Lambrecht, K.F. Brennan, *J. Appl. Phys.* **86**, 6864 (1999).
13. O.P. Malyk, *Comput. Mater. Sci.* **33** No 1-3, 153 (2005).
14. O.P. Malyk, *Physica B* **404** No 23-24, 5022 (2009).
15. O.P. Malyk, *Can. J. Phys.* **92**, 1372 (2014).
16. O.P. Malyk, *J. Nano- Electron. Phys.* **14** No 5, 05007 (2022).
17. W. Voigt, *Lehrbuch der Kristallphysik* (Teubner, Leipzig, 1910, reprinted 1928).
18. O.P. Malyk, *J. Alloy. Compd.* **371**, No 1-2, 146 (2004).
19. W.N. Lawless, T.K. Gupta, *J. Appl. Phys.* **60**, 607 (1986).
20. R.A. Robie, H.T. Haselton Jr., B.S. Hemingway, *J. Chem. Thermodynamics* **21**, 743 (1989).

Ab initio обчислювальна схема для опису кінетичних властивостей вюртцитного оксиду цинку

О.П. Малик

Національний університет «Львівська політехніка», 29013 Львів, Україна

У цьому дослідженні вперше запропоновано методологію, засновану на принципах ab initio, для визначення кінетичних характеристик вюрцитного оксиду цинку. Транспортні властивості матеріалу аналізуються за допомогою ретельно розроблених близькодіючих моделей взаємодії, які враховують процеси розсіювання електронів, викликаних різними типами кристалічних дефектів. В рамках теорії функціоналу густини (DFT) ймовірності переходів для розсіювання електронів на дефектах кристалічної решітки були визначені з використанням чисельно отриманих власних функцій разом із самоузгодженим кристалічним потенціалом. Цей підхід дозволив виключити параметри підгонки для шести механізмів розсіювання електронів. Окреслено вибір псевдопотенціалів цинку та кисню, що забезпечує покращену узгодженість між теоретичними та експериментальними кінетичними характеристиками ZnO в діапазоні температур від 3 до 400 K. Було доведено, що близькодіючі моделі відтворюють експериментальні результати точніше, ніж далекодіючі моделі.

Ключові слова: Вюрцитний оксид цинку, Хвильова функція DFT, Електронний транспорт, Точкові дефекти.